Preprints of the 21st IFAC World Congress (Virtual)
Berlin, Germany, July 12-17, 2020

A new controllability index based on Hankel singular value ⋆

Shuanghua Yang * **Wolfgang Birk** ** **Yi Cao** ***

* *College of Chemical and Biological Engineering, Zhejiang University, China & Institute of Zhejiang University-Quzhou, Quzhou, China (e-mail: yangsh@zju.edu.cn)*
** *Control Engineering Group, Luleå University of Technology, Sweden(e-mail: wolfgang@ltu.se)*
*** *College of Chemical and Biological Engineering, Zhejiang University, China, & Institute of Zhejiang University-Quzhou,Quzhou,China (e-mail: caoyi2018@zju.edu.cn)*

Abstract:
This paper proposes a new controllability index based on the Hankel singular values (HSV) which is applicable for both single-input single-output (SISO) and multivariable processes. The new index quantifies the inherent performance limitation in terms of closed-loop response speed by associating it with the control effort, which is directly related to the inverse of the HSVs. It is also shown that for specific system there is a direct linear relationship between the inverse of the minimum Hankel singular value and desired closed loop pole locations. The controllability index is thereafter exemplified on several SISO examples systems to show some of its properties. Thereafter two well-known multivariable benchmark processes, quadruple tank and two-continuous-stirring-tank-reactor are used to show the effectiveness of the index. It is concluded that the index provides valuable insights to practitioners on the achievable performance of processes with actuator constraints, while being easy to use and requiring little computational effort.

Keywords: Hankel Singular Value, Gramian, Input-Output Controllability Analysis, Inherent Performance Limitation, Pole Placement

1. INTRODUCTION

Digitalization, together with the Industry 4.0 paradigm is leading to a radical change in the engineering and operation of industrial systems, meaning industrial automation needs to evolve and adopt a customer oriented business mode. In this mode, production and manufacturing systems have to respond to customer specified orders very quickly requiring to alter operating conditions regularly. For industrial systems with relatively large time constants while being constraint in their actuation capabilities, the requirement to quickly change operating conditions poses new challenges to the engineering of industrial control systems. In essence, control engineers simply need to have a clear understanding what the inherent performance limitation on the closed-loop response speed is.

Introduced by Morari et al. (1980), inherent control performance limitation, referred to as controllability, or input-output controllability to differentiate it from the conventional state controllability, was identified having three main causes, namely manipulated variable constraints, non-minimum phase characteristics imposed by right-half-plane zeros and time-delays, and plant-model mismatches. Optimization problems can be formulated to quantify limitations in these aspects, *e.g.* (Cao et al., 1996). However, to facilitate process and control designs, simple controllability indicators are more desired by practicitioner. Many controllability indicators have been proposed and studied in the literature, such as the minimum singular value and its alternatives to quantify input constraints (Cao and Biss, 1996), pole and zero directions to quantify non-minimum phase behaviours (Skogestad and Postlethwaite, 1996) and the minimum condition number to evaluate the effect of uncertainties on performance limitation (Skogestad and Postlethwaite, 1996), just to mention a few. Many tools have been developed to use these controllability indicators for control structure design (Cao and Biss, 1997; Cao and Saha, 2005; Cao and Kariwala, 2008).

The closed-loop response speed requirement can be converted into a pole placement region. For all closed-loop poles in this region is equivalent to a set of linear matrix inequalities derived by Chilali and Gahinet (1996). This result together with other design requirements are adopted for multiple-objective controllability analysis in (Cao and Yang, 2004). Nevertheless, the nature of LMIs creates a trade-off between input H_2 norm and pole placement, and makes the algorithm too complicated to be suitable for screening a large number of control structure candidates.

In this work, a new Gramian based controllability index is proposed to link the closed-loop response speed limitation

⋆ The work is supported by the National Key Research and Development Plan (2017YFC1502902) of P. R. China.

with manipulated variable constraints, directly. The new index is based on the Hankel singular value (HSV) theorem proven by Glover (1986), which states that the minimum control effort for a controller to stabilize a linear unstable system is the inverse of minimum HSV of the unstable projection of the system under control. In this work, the theorem is extended to stable systems by shifting the imaginary axis to reflect closed-loop pole displacement, hence, reflecting closed-loop response speed requirement. Numerical examples are used to show this new index indeed is able to quantify the dependence of closed-loop response speed on the control effort, which is limited due to manipulated variable constraints. Conventionally, a stable pole is not considered inducing any control limitation. However, the new index does reveal that the stable pole location together with manipulated variable constraint imposes a limitation on the achievable closed-loop speed.

The work is organised as follows, after introduction, the preliminary of HSV theorem is presented in section 2. Then, the new controllability index is proposed by extending the HSV theorem in section 3. Section 4 presents several numerical examples using the new controllability index. Finally, the work is concluded in section 5.

2. HANKEL SINGULAR VALUE THEOREM

Glover (1986) has proven that the minimum input usage to stabilize an unstable plant can be quantified by the minimum HSV of the anti-stable projection of the plant.

Let $G = \{A, B, C\}$ be a linear system with n_x states, n_u inputs and n_y outputs, where A, B, and C are state, input and output matrices with corresponding dimensions, respectively. The controllability and observability Gramians, L_c and L_o of the system are symmetric and can be determined by the solution of the Lyapunov equations, respectively, as follows.

$$AL_c + L_cA^T + BB^T = 0 \tag{1}$$

$$A^TL_o + L_oA + C^TC = 0 \tag{2}$$

The HSVs, $\underline{\sigma} = \sigma_1 \leq \sigma_2 \cdots \leq \sigma_{n_x} = \bar{\sigma}$ of the system are defined as follows,

$$\sigma_k(G) = \sqrt{\lambda_k(L_oL_c)}, \quad k = 1, 2, \ldots, n_x \tag{3}$$

If the system is unstable, then the system can be decomposed into stable (G_s) and anti-stable (G_a) projections, *i.e.*, $G = G_s + G_a$ (Safanov et al., 1987). Glover (1986) indicated that the minimum control effort for a controller, K to stabilize $(G + \Delta)$ for all allowable perturbations Δ is the minimized norm of $\|KS\|_\infty$, where $S := (I - GK)^{-1}$. The minimum norm can be calculated as follows (Glover, 1986):

$$\min \|KS\|_\infty = \frac{1}{\underline{\sigma}([G_a(-s)]^*)} \tag{4}$$

In the next section, the HSV theorem is to be extended to stable systems to derive a new controllability index.

3. CONTROLLABILITY INDEX

The HSV theorem established the relation between the input usage and stabilization. Input usage is an important controllability factor, which indicates whether or not a required control task is achievable due to input saturations. It is also well-known that the closed-loop response is predominantly determined by closed-loop pole locations. In order to ensure a sufficiently fast response, the closed-loop poles have to be allocated on the left-hand side of a certain point on the s-plane. More specifically, if the closed-loop response is required at least as fast as $e^{-\alpha t}$, then the real parts of all closed loop poles, $p_i, i = 1, \ldots, n_x$, have to satisfy $\text{real}(p_i) \leq -\alpha$.

This problem can be converted to a stabilization problem by introducing a shift of the imaginary axis of the s-plane to $s = -\alpha$. Thus, requiring a stable closed loop system for the shifted imaginary axis, renders fulfillment of the performance specification. In addition, there is no need to specify exact pole locations, but instead an easily specified minimum requirement on the closed loop response speed. Most importantly, the HSV theorem can now be extended to link the input usage and the closed-loop response speed.

Assume the controller K is to produce closed-loop response converging faster than $e^{-\alpha t}$. Then the corresponding closed-loop poles have to be allocated on the left-hand side of the vertical line of $s = -\alpha$ on the s-plane. By shifting the $j\omega$ axis to $s = -\alpha$, the new plane is $s' = s + \alpha$, or $s = s' - \alpha$. The closed-loop pole allocation problem is then equivalent to the stabilization problem on the new s' plane. Since $sI - A = s'I - A'$, where $A' = A + \alpha I$, the HSV theorem can be extended as follows.

Let $G' = \{A', B, C\}$, G'_s and G'_a are stable and anti-stable projections of G', *i.e.* $G' = G'_s + G'_a$. Then, the minimum control effort needed to have the closed-loop response faster than $e^{-\alpha t}$ can be determined as follows.

$$\min \|KS'\|_\infty = \frac{1}{\underline{\sigma}([G'_a(-s)]^*)} \tag{5}$$

where $S' := (I - G'K)^{-1}$ and S' depends on α.

If G is properly scaled such that the maximum allowable input magnitude is one, then feasible pole locations in terms of α are given for $\|KS'\|_\infty \leq 1$ for all permissible uncertainties, such as the difference between initial condition and steady-state. This factor makes the minimum HSV calculated as above an appropriate controllability index. The pole location corresponding to $\underline{\sigma}([G'_a(-s)]^*) = 1$ gives the performance limitation on response speed.

For integrated process and control design, it is desired to compare performance limitations of different designs. For such a task, the minimum input norm, $\min \|KS'\|_\infty$, can be plotted against the pole shift α to a desired location, such that further adjustment or comparison of different designs can be concluded easily. Nevertheless, in oder to determine feasible values for α, a one dimensional search has to be performed.

For a special case, where only one real pole, p is on the right-side-half plane of the vertical line, $s = -\alpha$, then the minimum input norm, $\min \|KS'\|_\infty$ is a linear function of the shifting distance, α. This can be proven as follows. Since G'_a have only one ploe, both state matrix A and Gramians L_c and L_o are scalar. Hence, equation (1) can be simplified as

$$2AL_c + BB^T = 0 \tag{6}$$

Shifting A with $-\alpha$ gives the new Gramian as $L_c' = L_c + \delta_c$ satisfying

$$2(A+\alpha)(L_c+\delta_c) + BB^T = 0 \tag{7}$$

Combining (6) and (7) gives

$$\delta_c = -\frac{\alpha L_c}{A+\alpha} \tag{8}$$

For (2), defining $L_o' = L_o + \delta_o$ leads to as follows.

$$\delta_o = -\frac{\alpha L_o}{A+\alpha} \tag{9}$$

Furthermore,

$$L_o' L_c' = (L_o+\delta_o)(L_c+\delta_c) = L_o L_c \left(1 - \frac{\alpha}{A+\alpha}\right)^2$$

Hence, the HSV of the shifted system is derived as follows.

$$\sigma' = \sqrt{\lambda(L_o' L_c')} = \sigma\left(1 - \frac{\alpha}{A+\alpha}\right) = \sigma\left(\frac{A}{A+\alpha}\right) \tag{10}$$

The minimum input norm of the shifted system is then

$$\min \|KS'\|_\infty = \frac{1}{\sigma'} = \frac{1+\alpha/A}{\sigma} = \min \|KS\|_\infty (1+\alpha/A)$$

To conclude

$$\min \|KS'\|_\infty = \min \|KS\|_\infty + \frac{\min \|KS\|_\infty}{A}\alpha \tag{11}$$

This means for a single real pole, the minimum input norm will increase as the shifting distance increase with a slope of $\frac{\min \|KS\|_\infty}{A}$. Hence, it is not necessary to calculate the entire curve of input norm against the shifting distance, but only at one shifting point of $A = \alpha_0$, to calculate the corresponding $\min \|KS\|_\infty$. Then, the entire curve can be obtained using (11).

The shifting has to be on the left of the rightmost open-loop pole. This is because if the desired closed-loop pole location corresponding to the desired response speed is on the right of the rightmost pole, then it means the time constant of the open loop system is small enough to achieve desired response speed without any concerns. Thus, for the one dimensional search, the initial value for α can be chosen close to, but not equal to (to avoid $A = 0$ in (11)), the right most pole location of the open-loop system in the left half plane, and thereafter iterating towards $-\infty$.

To conclude, the controllability index provides a link between the response speed and control input magnitude. Therefore, by checking the function of the control effort against the pole location, an engineer can design an appropriate input saturation, namely dimensioning of the actuators, based on required closed-loop response speed.

4. EXAMPLES

In order to exemplify the usage of the new controllability index a number of examples are used. First some numerical examples for single-input and single-output (SISO) systems are used to show the characteristics of the input magnitude in relation to the pole shift for the cases of systems with individual real poles, systems contain complex conjugate poles and poles with multiplicity.

Thereafter, the quadruple tank process and the two-continuous-stirring-reactor (2-CSTR) process are used to show the feasibility for multivariable processes and how the

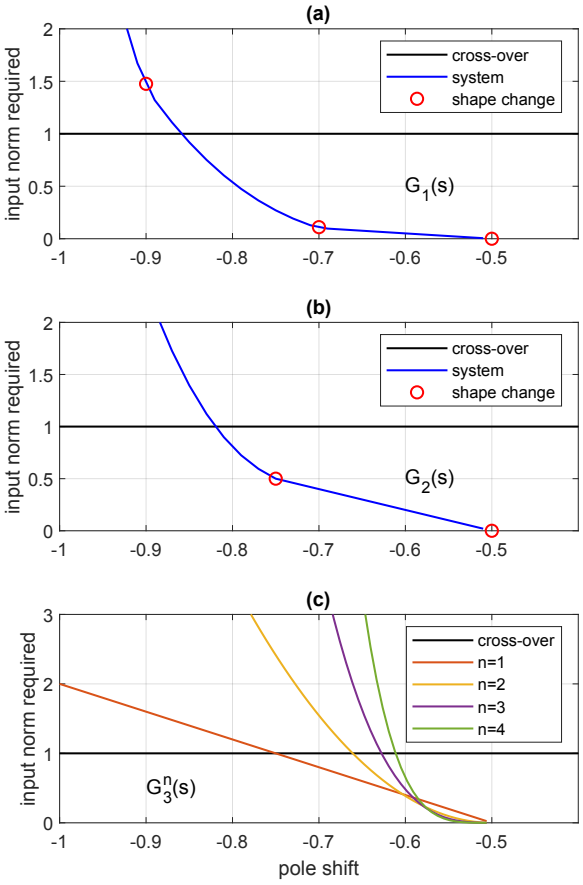

Fig. 1. Controllability index against pole shifts for three SISO systems

effect of interactions can be observed using the proposed controllability index. These two examples exhibit different characteristics, as there are input constraints depending on operating conditions.

4.1 SISO systems

Three SISO systems with individual real poles, complex poles and multiple real poles are considered as follows.

$$G_1(s) = \frac{0.315}{(s+0.9)(s+0.7)(s+0.5)} \tag{12}$$

$$G_2(s) = \frac{0.5}{(s+0.5)(s^2+1.5s+1)} \tag{13}$$

$$G_3(s) = \frac{1}{(2s+1)^n} \tag{14}$$

The new controllability index is calculated for these three systems for different pole shifts and is depicted in Fig. 1.

For the system with real poles (12), shown in Fig. 1a, it can be seen that the shape of the curve representing the relationship between the input norm and the pole shift is changing at the individual pole locations. Between the pole location -0.5 and -0.7, the curve adheres a linear curve in accordance with (11), whereafter a higher order trend is adhered. It can also be concluded that the poles can be shifted up to -0.86, where the input norm reaches the magnitude 1, rendering actuator saturation.

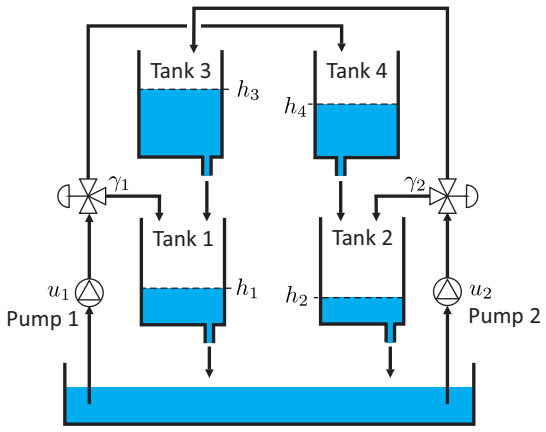

Fig. 2. Quadruple tank system

Similarly, for the system with complex poles (13), where the complex pole pair is located at $(-0.75 \pm j0.6614)$, shown in Fig. 1b, change in the shape of the relationship can be observed at -0.75, where the linear curve changes into a higher order trend. It can also be observed that a pole shift to -0.82 would be possible, but beyond that point actuator saturation can be expected, rendering a performance limitation. Moreover, the behaviour can be considered consistent with $G_1(s)$.

For the system with repeated real poles (14), with n indicating the multiplicity of the pole at $-1/2$, shown in Fig. 1c, it is well known that increased values of n do reduce the responsiveness of the system and a requirement on reduced response times of the closed loop system will render increased values for the input norm. There it can be seen that the required input norm for a faster response is increasing rapidly with the increased multiplicity of the poles of the system. Moreover, it can be seen that the single pole case results in a linear relation with the pole shift α.

4.2 Quadruple tank process

The quadruple-tank (QT) is an interacting system where two pumps deliver their flow to four interconnected tanks as depicted in Fig. 2 and discussed in Johansson (2000). The inputs u_j are the voltage applied to pump j, and the outputs h_i are the level in tank i. The flow from the pumps is then split into two flows using the ratio γ_j set by the respective split valve. The linearized model is known to be

$$G(s) = \begin{bmatrix} \dfrac{\gamma_1 c_1}{1+sT_1} & \dfrac{(1-\gamma_2)c_1}{(1+sT_3)(1+sT_1)} \\ \dfrac{(1-\gamma_1)c_2}{(1+sT_4)(1+sT_2)} & \dfrac{\gamma_2 c_2}{1+sT_2} \end{bmatrix} \quad (15)$$

where $T_i = \frac{A_i}{a_i}\sqrt{2h_i^0/g}$ are the time constants of the tanks, h_i^0 is the level of the tank i at the considered working point and $c_i = T_i k_i / A_i$. The considered process parameters are summarized in Table 1. For the assessment of the new controllability index the operating point as described in Table 2 is used.

The controllability index can now be calculated for a range of pole shifts which represent potential performance

Table 1. QT process parameters.

Parameter	Value	Description
A_1, A_3	28 cm^2	Cross section of tanks 1 and 3
A_2, A_4	32 cm^2	Cross section of tanks 2 and 4
a_1, a_3	0.071 cm^2	Area of the bottom hole of Tanks 1, 3
a_2, a_4	0.057 cm^2	Area of the bottom hole of Tanks 1, 3
g	981 cm/s^2	Gravity acceleration
k_1	3.33	Flow from Pump 1 for a voltage unit
k_2	3.35	Flow from Pump 1 for a voltage unit
γ_1	0.59	Flow fraction from Pump 1 into Tank 1
γ_2	0.45	Flow fraction from Pump 1 into Tank 2

Table 2. QT operating conditions

Variable	u_1^0	u_2^0	h_1^0	h_2^0	h_3^0	h_4^0
Value	3 V	3.2 V	14.1 cm	12.5 cm	3.5 cm	2.6 cm

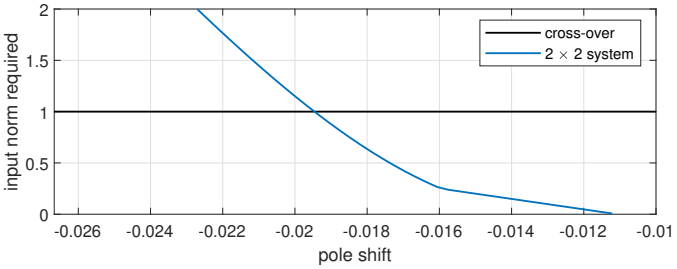

Fig. 3. Controllability index for a range of pole shifts of the complete quadruple tank process

requirements. In Fig . 3, the controllability index for the complete quadruple tank process is shown. There it can be seen that pole shifts of up to -0.02 can be considered before the closed loop system would exhibit actuator saturations. Interestingly, in Fig. 4, when assessing the controllability index for the individual subsystems of the quadruple tank, it can be seen that the possible pole shift is exceeding -0.02. Thus, the interaction effect in the quadruple tank limits the attainable performance for a closed loop control system significantly. The depicted trends can also be confirmed with the shifted input norm equation derived in (11). The difference in behaviour of the individual subsystems and for the complete process also motivates the question if and how a control structure design could be determined on the basis of the difference. A future study should investigate that research question.

4.3 Two continuous stirring tank reactor process

Consider the two stage continuous stirring tank reactor system, shown in Fig. 5. An eight-state nonlinear model of the system was presented in (Cao et al., 1996). The model was then reduced to six states by assuming constant volumes in both reactors in (Cao and Yang, 2004). The 6-state model is adopted in this work. Three possible control configurations are considered in (Cao and Yang, 2004):

S1: $u = [Q_{I1}, Q_{I2}]^T$, two feed flowrates and $y = [T_{o1}, T_{o2}]^T$, two tank outlet temperatures. To cope with the input constraint $0.05 \leq Q_{I1} + Q_{I2} \leq 0.8$ [m^3/s], these inputs are converted to total throughput, $Q_I = Q_{I1} + Q_{I2}$ and second inlet ratio, $R_2 = Q_{I2}/Q$, *i.e.* $u = [Q_I, R_2]^T$.

S2: $u = [Q_{cw1}, Q_{cw2}]^T$, two cooling-water flowrates and y is the same as S1.

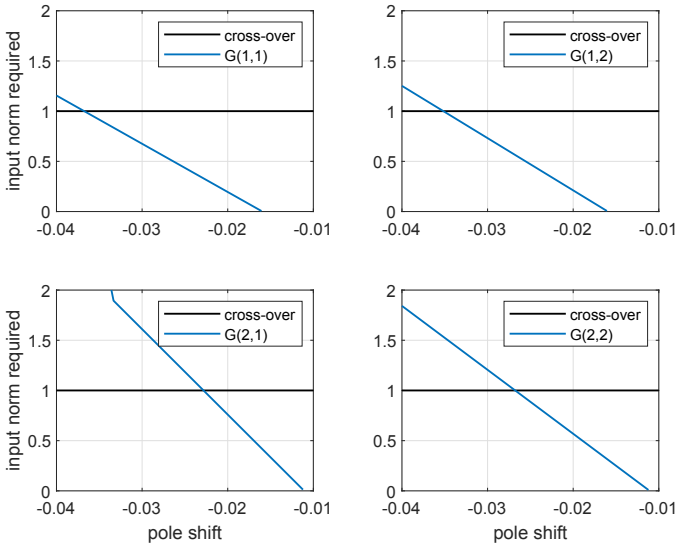

Fig. 4. Controllability index for a range of pole shifts of the individual transfer functions in the transfer matrix of the quadruple tank

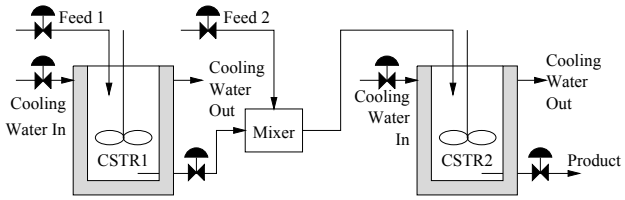

Fig. 5. Two stage CSTR system

S3: u is the same as S2, but y has two extra secondary measurements, cooling-water outlet temperatures, i.e. $y = [T_{o1}, T_{o2}, T_{cwo1}, T_{cwo2}]^T$.

After appropriate input and output scaling to consider both input constraints and operating range, the linear state space models of these configurations adopted from (Cao and Yang, 2004) are as follows

$$\dot{x} = Ax + B_i u, \quad y = C_i x \tag{16}$$

where B_i and C_i are B and C matrices for configurations $\mathbf{S}i$, respectively.

$$A = \begin{bmatrix} -17.9751 & -295.8655 & 0 & 0 & 0 & 0 \\ 0.0207 & 0.1889 & 0.0704 & 0 & 0 & 0 \\ 0 & 0.3879 & -0.8000 & 0 & 0 & 0 \\ 0.0977 & 0 & 0 & -18.0088 & -295.8655 & 0 \\ 0 & 0.0617 & 0 & 0.0131 & 0.0433 & 0.0589 \\ 0 & 0 & 0 & 0 & 0.3787 & -0.6220 \end{bmatrix} \tag{17}$$

$$[\,B_1 | B_2\,] = \left[\begin{array}{cc|cc} 17.8996 & -13.7811 & 0 & 0 \\ -0.0131 & 0.0101 & 0 & 0 \\ 0 & 0 & -0.0294 & 0 \\ 17.8636 & 17.8636 & 0 & 0 \\ -0.0082 & -0.0082 & 0 & 0 \\ 0 & 0 & 0 & -0.0235 \end{array}\right] \tag{18}$$

$$B_3 = B_2 \tag{19}$$

$$C_3 = \left[\begin{array}{cccccc} 0 & 362.9950 & 0 & 0 & 0 & 0 \\ 0 & 0 & 0 & 0 & 362.9950 & 0 \\ \hline 0 & 0 & 327.5600 & 0 & 0 & 0 \\ 0 & 0 & 0 & 0 & 0 & 335.4470 \end{array}\right] \tag{20}$$

$$C_1 = C_2 = \text{ the first two rows of } C_3 \tag{21}$$

Open-loop poles and transmission zeros of these configurations are listed as follows.

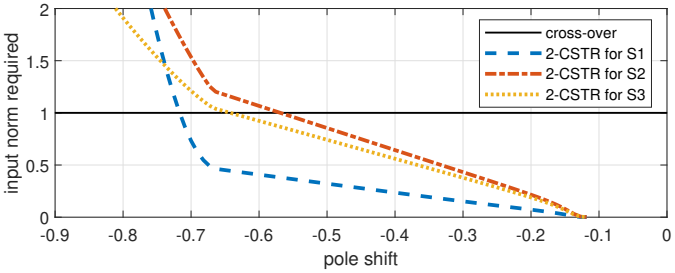

Fig. 6. Minimum input norm of three control configurations of the 2-CSTR system versus closed-loop pole location requirement.

poles: $-17.8,\ -17.6,\ -0.84,\ -0.67,\ -0.13\ -0.11$

zeros of S1: $10.33,\ 10.31,\ -0.8,\ -0.62$

zeros of S2: $-18.01,\ -17.98$

zeros of S3: none

Note, configuration S3 is a non-square system, hence does not have any transmission zeros. It is included in this work on purpose to investigate how the new controllability index works for non-square systems. After calculating the new controllability index, results of the minimum control effort required against desired closed-loop pole location for these three configurations are shown in Fig. 6

In Fig. 6, non-zero input norm values for all configurations start from the rightmost open-loop pole, $\alpha = -0.11$. These norm curves change their slopes at the second rightmost pole $\alpha = -0.13$, but the change is too close to the first right pole to be observed clearly. At the third rightmost pole, $\alpha = -0.67$ these curves have another change of slopes. Other changes are beyond the range of the graph, and hence, not observable. It is interesting to see that although the first scheme **S1** has two non-minimum phase zeros, requires the least input norm amongst these three schemes. A theoretical explanation of this counter-intuitive behaviour will be subject to future research. Finally, the non-square configuration, **S3** with extra secondary measurements, does improve controllability from the **S2** configuration by extending the feasible closed-loop pole range with the given input constraints. These results are consistent with those concluded from the multi-objective controllability analysis conducted in (Cao and Yang, 2004), where a much more complicated algorithm, solving several linear matrix inequalities was adopted. Therefore, the simplicity of the proposed controllability index in this work is very compelling and better suited for the design of control policy, and particularly to screen a large number of possible policies.

Using a nonlinear closed-loop dynamic simulation the predictions by the controllability index are cross-verified. Both T_{o1} and T_{o2} loops are controlled by PI controllers for both **S1** and **S2** configurations. For **S3**, a distributed cascade control configuration is adopted, where T_{cwo1} and T_{cwo2} are treated as secondary controlled variables and controlled by proportional controllers in addition to the primary controlled variables, T_{o1} and T_{o2}, controlled by PI controllers, respectively. Controller parameters are shown in Table 3. Nonlinear closed-loop simulations are conducted for tank temperature set points change by $\pm 0.1K$, respectively. The simulation results for the output

Table 3. 2-CSTR controller parameters

	T_{o1}		T_{o2}		T_{cwo1}	T_{cwo2}
	K_P	τ_I	K_P	τ_I	K_P	K_P
S1	0.5112	0.4764	0.7006	1.0395		
S2	−1.0824	3.9419	−0.9139	4.8641		
S3	68.5767	1.2337	56.6181	2.5045	−0.05	−0.05

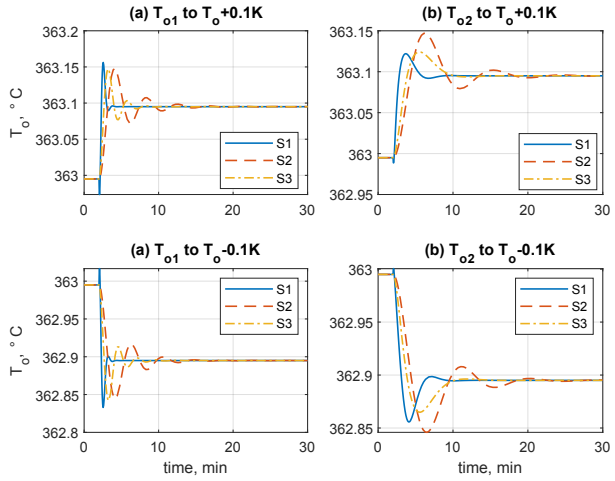

Fig. 7. Output responses to setpoint change by $\pm 0.1K$.

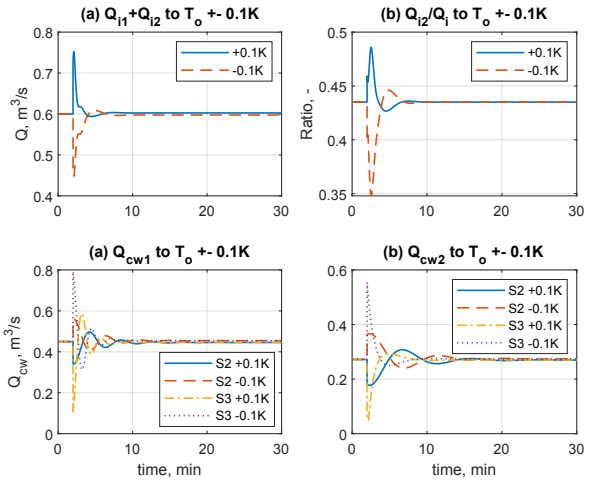

Fig. 8. Input responses to setpoint change by $\pm 0.1K$.

responses are shown in Fig. 7 and input responses in Fig 8. Fig. 7 shows that the response time with control scheme **S1** indeed is the shortest, followed by that of **S2**, then **S3**, while all inputs are not saturated as can be seen in Fig. 8. These results match the controllability ranking predicted by the new controllability index stated above.

5. CONCLUSIONS

A new controllability index to quantify the effect of input constraint on closed-loop response speed is proposed by extending the HSV theorem proven by Glover (1986). The original theorem was proven for unstable system. In the proposed extension, the imaginary axis of the s-plane is shifted according to closed-loop pole locations which determine the closed-loop response speed desired. The shifting of the pole location from open-loop poles to desired closed loop poles converts stable systems to unstable ones such that the HSV theorem can be applied. Numerical studies demonstrate the effectiveness of the new index despite its simplicity of use it does provide a reliable indication on achievable closed-loop response speed. It also provides an approach which is computational efficient.

Future work, will target efficient control structure design algorithms which can directly relate achievable closed loop performance with the selected control structure, motivated by the outcome of the quadruple tank process example. Moreover, the relationship between number of unstable poles and the curvature of the input magnitude curve depending on α is worth while investigating, which could imply the existence of a closed form solution for the input magnitude. Finally, the effect of zeros on the input norm need to be further investigated.

REFERENCES

Cao, Y. and Biss, D. (1996). An extension of singular value analysis for assessing manipulated variable constraints. *Journal of Process Control*, 6(1), 37–48.

Cao, Y. and Biss, D. (1997). An input pre-screening technique for control structure selection. *Computers and Chemical Engineering*, 21(6), 563–569.

Cao, Y., Biss, D., and Perkins, J.D. (1996). Assessment of input-output controllability in the presence of control constraints. *Computers and Chemical Engineering*, 20(4), 337–346.

Cao, Y. and Kariwala, V. (2008). Bidirectional branch and bound for control variable selection. *Computers and Chemical Engineering*, 32(10), 2306–2319.

Cao, Y. and Saha, P. (2005). Improved branch and bound method for control structure screening. *Chemical Engineering Science*, 60(6), 1555–1564.

Cao, Y. and Yang, Z.J. (2004). Multiobjective process controllability analysis. *Computers and Chemical Engineering*, 28(1–2), 83–91.

Chilali, M. and Gahinet, P. (1996). h_infty design with pole placement constraints: an lmi approach. *IEEE Transactions on Automatic Control*, 41, 358–367.

Glover, K. (1986). Robust stablization of linear-multivariable systems–relations to approximation. *International Journal of Control*, 43, 741–766.

Johansson, K. (2000). The quadruple-tank process: a multivariable laboratory process with an adjustable zero. *Control Systems Technology, IEEE Transactions on*, 8(3), 456 –465.

Morari, M., Arkun, Y., and Stephanopoulos, G. (1980). Studies in the synthesis of control structures for chemical process, Part I: Formulation of the problem. Process decomposition and the classification of the control tasks. Analysis of the optimizing control structures. *AIChE J.*, 26(2), 220–232.

Safanov, M., Jonckheere, E., Verma, M., and Limebeer, D. (1987). Synthesis of positive real multivariable feedback systems. *International Journal of Control*, 45(3), 817–842.

Skogestad, S. and Postlethwaite, I. (1996). *Multivariable Feedback Control: Analysis and Design*. John Wiley & sons, Chichester, UK, 1st edition.